Origami Hexagon Deformations and Flip Graph

July 2020

Abstract

We studied the collection of configurations of an isolated hexagon consisting of six equilateral triangles around a vertex on the triangular lattice. We quantitatively characterized the moduli space of deformations near the flat state. The rational and integer points on the deformation surface joining with flip operations admit a consistent combinatorial structure.

Contents

1 Introduction: Origami Hexagon

By utilizing origami folding processes, researchers have been able to solve a wide range of engineering problems such as fabricating different robot morphologies [1]. Leveraging origami structures in this way requires an understanding of the geometric and numerical properties of folding configurations. Given a fixed crease pattern, we want to know the folding configurations along those creases without curving the subplanes.

We are studying origami hexagon on triangular lattices, specifically, the collection of configurations of an isolated hexagon consisting of six equilateral triangles around a vertex on the triangular lattice as shown in Figure 1a. Figure 1b indicates the crease pattern of this isolated origami hexagon denoted by H. See some configuration examples in Figure 2.

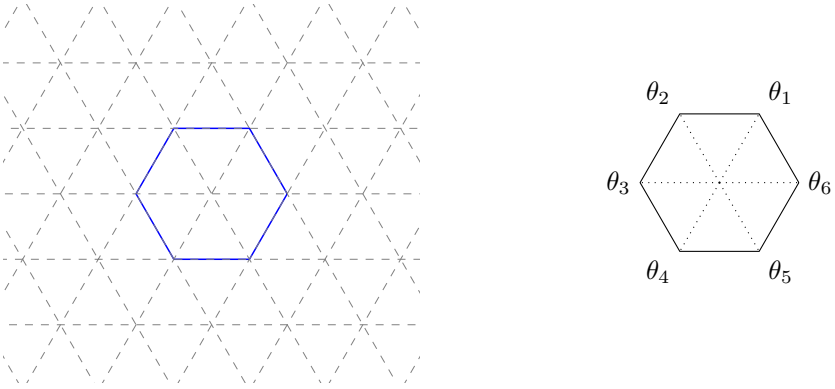

(a) Hexagon on triangular lattices (b) Isolated hexagon

Figure 1: Origami hexagon

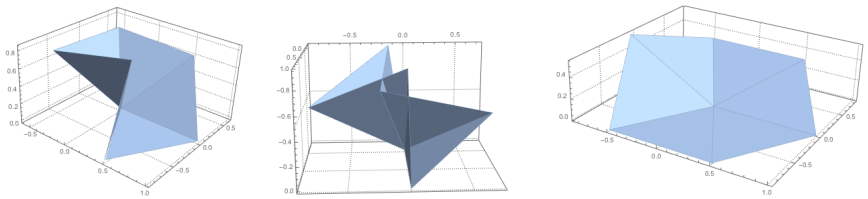

Figure 2: Hexagon configurations

In this paper, we quantitatively characterized this moduli space parameterized by six fold angles. By applying second order approximation, we obtained the moduli space of deformations near the flat state as the variety Y in $\mathbb{R}^6$,

$$Y = \begin{cases} x_5^2 = x_2^2 + 2x_1x_2 + 2x_2x_3 + 2x_1x_3 \\ x_1 + x_2 = x_4 + x_5 \\ x_2 + x_3 = x_5 + x_6. \end{cases}$$

There are six natural flip operations on the space Y, corresponding to a local change at each of the six folds on the hexagon. We created an acyclic directed graph from the action of these flip operations on integer-valued points of Y. This flip graph is analogous to the Calkin–Wilf tree. The vertices of Calkin–Wilf tree correspond one-to-one to positive rational numbers, with root 1 and two children of $\frac{a}{b}$ defined as $\frac{a}{a+b}$, $\frac{a+b}{b}$.

By considering rotations and reflections, the flip graph has connected components which are isomorphic to each other, where each component is graded. We gave out closed formulas for the number of vertices on each level and the number of mountain-valley configurations among them. By

generating the Markov transition matrix, we calculated the limiting distribution for mountain-valley configurations. On Pythagorean 4-tuples, there is an action by sign changes and the matrix A_4

$$A_4 = \begin{bmatrix} 0 & -1 & -1 & 1 \\ -1 & 0 & -1 & 1 \\ -1 & -1 & 0 & 1 \\ -1 & -1 & -1 & 2 \end{bmatrix},$$

which generates a graph that has a precise relation to the flip graph.

2 Moduli Space of A Hexagon

To understand geometric classification problems for origami hexagon H, we introduce coordinates on its moduli space and parameterize the collection. To describe the collection of configurations of H, we assign each configuration a quantity that could uniquely define it. A natural attempt of this quantity is this six-tuple

$$(\theta_1, \theta_2, \cdots, \theta_6), \theta_i \in \mathbb{R}/2\pi\mathbb{Z},$$

where each element corresponds to a supplementary angle of a dihedral angle between two intersecting equilateral triangle planes affiliated with the hexagon. As shown in Figure 1b.

The moduli space of the configuration collection is bounded by the hypercube $(\mathbb{R}/2\pi\mathbb{Z})^6$, with degrees of freedom 3 [4].

2.1 Moduli Space of Deformations

In the context of **near flat configurations**, each dihedral angle between two adjacent triangle planes is close to π, thus each θ_i is close to zero. By applying Taylor expansion and second order approximation, i.e., working in

$$\mathbb{Q}[\theta_i]/(\theta_i^2, \theta_i\theta_j), i \in \mathbb{Z}/6\mathbb{Z}, i \neq j,$$

we obtained an algebraic variety X in $\mathbb{R}^6$ [4]. By simplifying X in irreducible components, we change gear to another easier-to-understand algebraic variety Y,

$$Y = \begin{cases} x_5^2 = x_2^2 + 2x_1x_2 + 2x_2x_3 + 2x_1x_3 \\ x_1 + x_2 = x_4 + x_5 \\ x_2 + x_3 = x_5 + x_6. \end{cases} \tag{1}$$

More importantly, each solution satisfying Y is a valid configuration of origami hexagon H and each near flat configuration of hexagon H is a point on Y.

Claim 1. *Algebraic variety Y is the moduli space of deformations of the near flat state configurations.*

Proof. According to Chen and Santangelo, the space of deformations near the flat state is described by the null cone of some quadratic form [3]. For origami hexagon H, its moduli space has dimension 3. Thus we have such congruence,

$$\left\{\begin{matrix}\text{Near-flat configurations} \\ \text{of hexagon } H\end{matrix}\right\} \cong \left\{\begin{matrix}\text{Null cone of some quadratic} \\ \text{form } Q \text{ with dimension } 3\end{matrix}\right\} \tag{2}$$

Y is exactly described by the quadratic null cone inside $\mathbb{R}^4$ with actual dimension 3. We have showed that near-flat deformations are a subset of Variety Y. Then Y's

$$\mathbb{R}^6 \supset V^4 \cong \mathbb{R}^4$$

$$\supset Y \cong \begin{Bmatrix} \text{Null cone of some quadratic} \\ \text{form } Q \text{ with dimension } 3 \end{Bmatrix} \tag{3}$$

Combining Eq (2) and Eq (3), we conclude Y represents the moduli space of deformations near flat.

$$Y \cong \begin{Bmatrix} \text{Near-flat configurations} \\ \text{of hexagon } H \end{Bmatrix}$$

□

In the following context, we would refer Y as hexagon surface (near flat).
According to [4], Y has the same topological shape as quadratic form

$$x_1^2 + x_2^2 + x_3^2 - x_4^2 = 0,$$

which has signature $(3, 1)$. Y's topological shape Y is described by a product of spheres, $S^2 \times S^0$,

3 Rational Points on the Hexagon Surface

To characterize rational solutions of quadratic equations with rational coefficients, a geometric idea is that a line usually intersects a quadratic surface at two points because of the fundamental theorem of algebra. Then given a rational point $\mathcal{O}$ on a quadratic surface, we have such correspondence:

$$\{\text{Rational lines through } \mathcal{O}\} \cong \{\text{Rational points on this surface}\}.$$

Before we dive into the rational points on the hexagon surface, let's examine the rational parametrization for the quadratic surface $W^2 = Y^2 + 2XY + 2YZ + 2XZ$. It is a homogeneous form of $1 = y^2 + 2xy + 2yz + 2xz$, denoted as $\mathcal{C}$, with $x = \frac{X}{W}, y = \frac{Y}{W}, z = \frac{Z}{W}$. Suppose $\mathcal{O}$ is a rational point on $\mathcal{C}$, each rational line through $\mathcal{O}$ meets $\mathcal{C}$ in two rational points, $\mathcal{O}$ and $\mathcal{P}$. Conversely, each rational point $\mathcal{P}$ on $\mathcal{C}$ could form a ration line by joining $\mathcal{P}$ to $\mathcal{O}$. There is an one-to-one map from rational lines through O to all but one of the rational points on $\mathcal{C}$. To have a bijective map, we work in projective space.

3.1 Projective Space Interpretation

Consider curve $\mathcal{C} : w^2 = y^2 + 2xy + 2yz + 2xz$ on projective space $P^3(\mathbb{R})$, $\mathcal{C}$= $\{[x : y : z : w] | w^2 = y^2 + 2xy + 2yz + 2xz\}$.

We change the variables as $y = v - x - z$, resulting in $w^2 + x^2 + z^2 = v^2$. When $v = 0$, $(x, y, z, w) = (0, 0, 0, 0)$, which has no relative point on $P^3(\mathbb{R})$.

When v is nonzero, it is equivalent to working in affine space $\mathbb{R}^3$. We set $a = \frac{x}{v}, c = \frac{w}{v}, b = \frac{z}{v}$, then we obtain $a^2 + b^2 + c^2 = 1$, which passes through $(1, 0, 0)$. Given variables s, t, we have rational line L through $(1, 0, 0)$ as

$$L = \begin{cases} a - 1 = rm \\ b = sm \\ c = tm \end{cases}.$$

When $m = 0$, we have solution $(1, 0, 0)$. When $m \neq 0$,

$$m = \frac{-2r}{s^2 + t^2 - r^2}.$$

Then we have parametrization of (a,b,c) as

$$a = rm + 1 = \frac{s^2 + t^2 - r^2}{s^2 + t^2 + r^2}$$

$$b = sm = \frac{-2sr}{s^2+t^2+r^2}$$
$$c = tm = \frac{-2tr}{s^2+t^2+r^2}.$$

Tracing back, taking $v = s^2+t^2+r^2$, we have

$$x = s^2+t^2-r^2$$
$$y = 2r^2+2tr$$
$$z = -2tr$$
$$w = -2sr.$$

In conclusion, all pairs (s,t,r) one-to-one correspond to all rational lines through $(1,0,0)$, thus correspond to all rational points on quadratic surface $w^2 = y^2+2xy+2yz+2xz$.

With above parametrization,

$$\left\{\text{All the points on } P^2(\mathbb{R})\right\} \cong \left\{\begin{matrix}\text{All the rational points on} \\ \mathcal{C} \text{ on } P^3(\mathbb{R})\end{matrix}\right\}.$$

Claim 2. *The topological shape of the quadratic surface $w^2 = y^2+2xy+2yz+2xz$ on projective space $P^3(\mathbb{R})$ is a sphere.*

Proof. With changing variables, $w^2 = y^2+2xy+2yz+2xz$ is transformed into $w^2+x^2+z^2 = y^2$. If $w \neq 0$, this quadratic surface has the same topological shape as $y^2-x^2-z^2 = 1$ on $\mathbb{R}^3$, which are two half sphere.
If $w = 0$, we are equivalently working in $P^2(\mathbb{R})$, $x^2+z^2 = y^2$ has the shape as a circle.

This circle is attached to each half sphere, resulting in a complete sphere.

□

Claim 3. *The topological shape of Y on $P^3(\mathbb{R})$ is S^2.*

Proof. This is directly shown by Claim 2. □

3.2 Rational Parametrization

We want to find a bijective map from all the rational lines through some rational point on this hexagon surface to all rational points on the surface. Consider a 6-tuple $\theta_0 \in \mathbb{R}^6, \theta_0 = (\theta_1, \theta_2, \cdots, \theta_6), \theta_i \in \mathbb{R}$, satisfying

$$\theta_5^2 = \theta_2^2 + 2\theta_1\theta_2 + 2\theta_2\theta_3 + 2\theta_1\theta_3.$$

We have given out the rational parametrization for this quadratic form above as

$$\theta_1 = s^2+t^2-r^2$$
$$\theta_2 = 2r^2+2tr$$
$$\theta_3 = -2tr$$
$$\theta_5 = -2sr.$$

With 2 linear constraints

$$\theta_4 = \theta_1+\theta_2-\theta_5$$
$$\theta_6 = \theta_2+\theta_3-\theta_5,$$

we obtain the complete rational patametrization

$$\begin{aligned}\theta_1 &= s^2 + t^2 - r^2\\ \theta_2 &= 2r^2 + 2tr\\ \theta_3 &= -2tr\\ \theta_4 &= s^2 + t^2 + 2tr + 2sr + r^2\\ \theta_5 &= -2sr\\ \theta_6 &= 2r^2 + 2sr.\end{aligned}$$

Claim 4 (Real Solutions' Approachability)**.** *For each real tuple $\theta = (\theta_1, \theta_2, \cdots, \theta_6), \theta_i \in \mathbb{R}$ on the hexagon surface, there exists a sequence $\{R_n\}$ satisfying Y that approaches θ.*

Proof. All the parametrization functions for $(s, t, r) \in \mathbb{R}^3$ on RHS are continuous, indicating for any real solution on the hexagon surface we could approach it with a rational solution sequence. □

3.3 Flip operation

Observation 1. *If $(x, y, z) \in \mathbb{R}^3$ satisfies*

$$0 = Q(x, y, z) = y^2 + 2xy + 2xz + 2yz = 0,$$

then

$$0 = Q(2y + x, -y, 2y + z).$$

Points on the hexagon surface has the same transition invariant above. When we change one crease to its opposite direction with the same fold angle value, and add two times the original value to its neighbors, the new point is still on this hexagon surface. We consider this inter-set transition as a *flip operation*.

There are six natural *flip operations* on the space Y, corresponding to a local change at each of the six folds on the hexagon.

Definition 1. *A **flip operation** applied on a fold angle θ_i is a function $F_i : \mathbb{R}^6 \to \mathbb{R}^6$, such that*

$$\begin{aligned}\theta_{i-1} &\to \theta_{i-1} + 2\theta_i\\ \theta_{i+1} &\to \theta_{i+1} + \theta_i\\ \theta_i &\to -\theta_i\end{aligned}$$

$$F_i(\theta_1, \theta_2, \cdots, \theta_6) = (\cdots, \theta_{i-1} + 2\theta_i, -\theta_i, \theta_{i+1} + 2\theta_i, \cdots)$$

F_i is associated with matrix M_i,

$$\begin{pmatrix} 1 & & & & & & \\ & \ddots & & & & & \\ & & 1 & 2 & & & \\ & & & -1 & & & \\ & & & 2 & 1 & & \\ & & & & & \ddots & \\ & & & & & & 1 \end{pmatrix}$$

For example, F_2 maps configurations as follows:
Note that the inverse of F_i has the same matrix as M_i, thus $F_i^{-1} = F_i$.

Proposition 1. *Suppose two six-tuples θ, γ are connected by a flip operation F_i, i.e. $F_i(\theta) = \gamma$. If θ is a valid hexagon configuration, i.e. satisfying variety Y, so does γ.*

Proof. This is directly deduced by Observation 1 and Claim 1. □

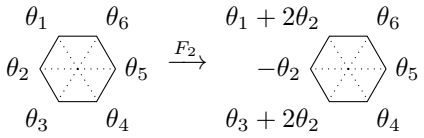

Figure 3: Flip operation

4 Integer Points and Flip Graph

Rational solutions are representing the practical crease angles, where it is natural to correspond rational points on the hexagon surface to physical configurations. The set of rational solutions measures near flat configurations in external world. Intuitively, to reflect the internal relationships of near flat configurations, we change gear to integer points on the hexagon surface. In the following context, we are studying primitive integer $6-$tuple $(\theta_1, \theta_2, \cdots, \theta_6)$ satisfying Y,

$$\theta_5^2 = \theta_2^2 + 2\theta_1\theta_2 + 2\theta_2\theta_3 + 2\theta_1\theta_3$$

$$\theta_1 + \theta_2 = \theta_4 + \theta_5$$
$$\theta_2 + \theta_3 = \theta_5 + \theta_6.$$

A noteworthy character for the set of integer configurations is we don't have any valid $6-$tuple with $\sum_i \theta_i = 0$. We would prove this later.

$\sum \theta_i$ is such an important character for a configuration that it deserves a name, ***complexity***. We classify integer configurations by the sign of $\sum \theta_i$, there are some properties regarding to the partial sum of fold angles.

Proposition 2. *Suppose $(\theta_1, \theta_2, \cdots, \theta_6)$ is a valid integer configuration with $\sum \theta_i > 0$, then*

(a) $\theta_i + \theta_{i+1} \geq 0$

(b) $\theta_{i-1} + \theta_i + \theta_{i+1} > 0$

(c) $\theta_{i-1} + \theta_i + \theta_{i+1} \geq -2\theta_i$

Proof. We will prove the second statement first.

(b). If there exists three consecutive angles with a non-positive sum, without loss of generality, suppose $\theta_1 + \theta_2 + \theta_3 \leq 0$. We have mentioned above that $\theta_5^2 = \theta_2^2 + 2\theta_1\theta_2 + 2\theta_2\theta_3 + 2\theta_1\theta_3$, adding θ_1^2, θ_3^2 on both sides, we have

$$\theta_1^2 + \theta_3^2 + \theta_5^2 = (\theta_1 + \theta_2 + \theta_3)^2 \tag{4}$$

When $\theta_1 + \theta_2 + \theta_3 \leq 0$,

$$\theta_1 + \theta_2 + \theta_3 = \theta_3 + \theta_4 + \theta_5 = \theta_5 + \theta_6 + \theta_1 = -\sqrt{\theta_1^2 + \theta_3^2 + \theta_5^2}$$

$$\sum \theta_i = -3\sqrt{\theta_1^2 + \theta_3^2 + \theta_5^2} - (\theta_1 + \theta_3 + \theta_5)$$

Since $a^2 + b^2 + c^2 \geq (a + b + c)^2/3$, we have the summation of all angles non-positive,

$$9(\theta_1^2 + \theta_3^2 + \theta_5^2) \geq (\theta_1 + \theta_3 + \theta_5)^2 \Rightarrow \sum \theta_i \leq 0,$$

which contradicts to the assumption. Thus $\theta_i + \theta_{i+1} + \theta_{i+2} > 0, \forall i$.

(a). Back to the first claim. If $\theta_i + \theta_{i+1} < 0$, without loss of generality, suppose $\theta_1 + \theta_2 < 0$, we have

$$\theta_1 + \theta_2 + \theta_3 = \pm\sqrt{\theta_1^2 + \theta_3^2 + \theta_5^2}.$$

Since we have proved that $\theta_1 + \theta_2 + \theta_3 > 0$,

$$\theta_1 + \theta_2 = \sqrt{\theta_1^2 + \theta_3^2 + \theta_5^2} - \theta_3 < 0$$

$$\Leftrightarrow \quad \sqrt{\theta_1^2 + \theta_3^2 + \theta_5^2} < \theta_3 \quad \Leftrightarrow \quad \theta_1^2 + \theta_5^2 < 0,$$

which is a contradiction. Thus, $\theta_i + \theta_{i+1} \geq 0, \forall i$.

(c). Without loss of generality, we could only check the case for $\theta_2 + 2\theta_3 + \theta_4 \geq -\theta_3$. Based on (b), and $a^2 + b^2 + c^2 \geq (a+b+c)^2/3$, we obtain

$$(\theta_1 + \theta_2 + \theta_3) + (\theta_3 + \theta_4 + \theta_5) = 2\sqrt{\theta_1^2 + \theta_3^2 + \theta_5^2} \geq \frac{2}{\sqrt{3}}(\theta_1 + \theta_3 + \theta_5) \geq \theta_1 + \theta_5 - \theta_3$$

$$\Leftrightarrow (\theta_2 + 2\theta_3 + \theta_4) + \theta_1 + \theta_5 \geq \theta_1 + \theta_5 - \theta_3$$

$$\Leftrightarrow \theta_2 + 2\theta_3 + \theta_4 \geq -\theta_3.$$

□

Notice that with symmetric proof, if $\sum \theta_i < 0$, we have $\theta_i + \theta_{i+1} \leq 0$ and $\theta_i + \theta_{i+!} + \theta_{i+2} < 0$.

Proposition 3. *Any primitive integer* 6*-tuple* $(\theta_1, \theta_2, \cdots, \theta_6)$ *satisfying* Y *has* $\sum_i \theta_i$ *either positive or negative.*

Proof. By Equation (4), if $\sum \theta_i = 0$,

$$\theta$$

□

Recall the flip operation we defined in Section 3.3. It is easy to see that flip operations preserve angles' belonging to congruence classes modulo 2. We claim that the sign of the summation of angles of a integer configuration would be preserved under flip operations.

Proposition 4. *For any two integer configurations connected by a flip operation described in Definition 1,*

$$(\theta_1, \theta_2, \cdots, \theta_6) \xrightarrow{F_j} (\theta_1', \theta_2', \cdots, \theta_6').$$

(a) $\sum \theta_i' = (\sum \theta_i) + 2\theta_j$.

(b) $\forall i, \theta_i \equiv \theta_i' \mod 2$.

(c) If $\sum \theta_i > 0$*, then* $\sum \theta_i' > 0$*. Similarly, if* $\sum \theta_i < 0$*, then* $\sum \theta_i' < 0$.

Proof. (a). Flipping angle θ_j, we have $\theta_{j-1}' = \theta_{j-1} + 2\theta_j, \theta_j' = -\theta_j, \theta_{j+1}' = \theta_{j+1} + 2\theta_j$,

$$\sum_i \theta_i' = (\theta_{j-1} + 2\theta_j) + (-\theta_j) + (\theta_{j+1} + 2\theta_j) + \theta_{j+2} + \theta_{j+3} + \theta_{j+4} = \sum_j \theta_j + 2\theta_j = \sum_i \theta_i + 2\theta_j.$$

(b). For the congruence classes mod 2,

$$\theta_{j-1}' \equiv \theta_{j-1} + 2\theta_j \equiv \theta_{j-1} \mod 2,$$

where the case is same for θ_{j+1}.

$$\theta_j' = -\theta_j \equiv \theta_j \mod 2.$$

(c). We only need to the case with $\sum \theta_i > 0$.

$$\sum \theta_i' = (\sum \theta_i) + 2\theta_j = (\theta_{j-1} + 3\theta_j + \theta_{j+1}) + (\theta_{j+2} + \theta_{j+3} + \theta_{j+4})$$

By Proposition 2(b), $\theta_{j+2} + \theta_{j+3} + \theta_{j+4} > 0$, and by Proposition 2(c), $\theta_{j-1} + 3\theta_j + \theta_{j+1} \geq 0$, thus,

$$\sum \theta_i' > 0.$$

□

4.1 Flip Graph

Creating graphs could provide a structural way to study a group. The Calkin-Wilf tree is an example providing an order of studying rational numbers.

Definition 2 (Calkin–Wilf Tree)**.** *The Calkin-Wilf tree is rooted at integer* 1*, and any rational number expressed in simplest terms as the fraction* $\frac{a}{b}$ *has as its two children the numbers* $\frac{a}{a+b}$ *and* $\frac{a+b}{b}$*.*

As shown in Figure 4a, the Calkin-Wilf is determined by a root and a children generating rule. The fascinating property of the Calkin-Wilf tree is

Every positive rational number appears exactly once in the tree.

Definition 3 (Flip Graph)**.** *Analogous to the Calkin-Wilf tree, we defined an acyclic directed graph, Flip graph G as follows:*

1. *G is rooted at primitive integer configurations with only positive or negative non-flat angles.*
2. *One primitive integer configuration* $\theta \in \mathbb{Z}^6$*, which is represented as a vertex in G, has its children generated by flip operation F with the following rules:*
   (a) *when* $\sum \theta_i > 0$*, the children of* θ *are* $\{F(\theta, \theta_i) | \forall \theta_i > 0\}$*,*
   (b) *when* $\sum \theta_i < 0$*, the children of* θ *are* $\{F(\theta, \theta_i) | \forall \theta_i < 0\}$*.*

Considering rotations and reflections, among primitive integer configurations, there are six configurations satisfying our definition for a valid root, which are the 3 rotations of $(0, 0, 1, 0, 0, 1)$ and 3 rotations of $(0, 0, -1, 0, 0, -1)$.

Figure 4b shows the first three layers of one component in Flip graph G rooted with $(0, 0, 1, 0, 0, 1)$.

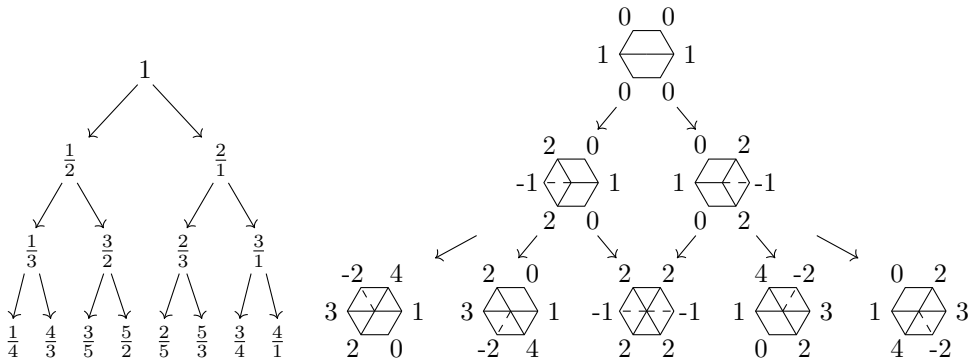

(a) The Calkin-Wilf Tree (b) Flip graph G

Figure 4: The Calkin-Wilf Tree and Integer configuration flip graph

From now on, we will be working with Flip Graph G and all the flip operations we refer to would be restricted to those defined in Definition 3 instead of the general ones.

Proposition 5. *Suppose* $\mathcal{P} = (\theta_1, \cdots, \theta_6)$ *is a valid primitive integer configuration with* $\sum \theta_i > 0$*. It has child* $\mathcal{C} = (\theta'_1, \cdots, \theta'_6)$ *by flipping fold angle* θ_j*. Then*

(a) $|\theta'_i| \geq |\theta_i|$*.*

(b) $|\theta'_{j+1}| \geq |\theta_j|, |\theta'_{j-1}| \geq |\theta_j|$*.*

(c) θ_j *is unique, i.e.* $\nexists k$ *s.t.* $F_k(\mathcal{P}) = \mathcal{C}, k \neq j$*.*

Proof. (a). We only need to check θ'_{j+1}. By Proposition 2(a), $\theta_j + \theta_{j+1} \geq 0$. Since Flip operation is processing on the positive angle, $\theta_j > 0$. Then

$$|\theta'_{j+1}| = |\theta_{j+1} + 2\theta_j| = |\theta_{j+1} + \theta_j| + |\theta_j| \geq |(\theta_{j+1} + \theta_j) - \theta_j| = |\theta_j|.$$

(b). It is sufficient to check θ'_{j+1} only. With the same reason above, $\theta_j + \theta j + 1 > 0, \theta_j > 0$, we have

$$|\theta'_{j+1}| = |\theta_{j+1} + 2\theta_j| = |\theta_{j+1} + \theta_j| + |\theta_j| \geq |(\theta_j|.$$

(c). Prove by contradiction. Suppose $\exists k$ satisfying the above condition. Then in $\mathcal{P}$, $\theta_k > 0$ and in $\mathcal{C}$, $\theta'_k < 0$. However, $\mathcal{C}$ is generated by $\mathcal{P}$ by flipping θ_j, which could not make any angle positive except θ'_j. It is contradicted to the transition from positive θ_k to negative θ'_k.

□

Claim 5. *Flip graph G is disconnected with six connected components which are isomorphic to each other.*

Proof. Based on the definition of Flip Graph G, we have roots with the following configuration: In

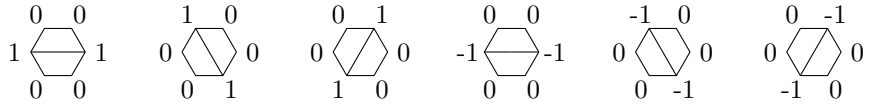

Figure 5: Roots for Flip Graph G

Proposition 5a, if $\sum \theta_i > 0$, the flip operation is defined on a positive angle, thus $\sum \theta'_i > 0$. Then we could conclude that all configurations generated from the rotation set of $(0, 0, 1, 0, 0, 1)$ must have positive complexity. The same situation applies to $(0, 0, -1, 0, 0, -1)$. Then each vertex in G connected to the rotation set of $(0, 0, 1, 0, 0, 1)$ cannot connect to the rotation set of $(0, 0, -1, 0, 0, -1)$. We have two disconnected components so far.

Now let's consider the configurations reached by the rotation set of $(0, 0, 1, 0, 0, 1)$. From Proposition 5b, the belongings to congruence classes modulo 2 are the same if two vertices are connected, which shows every vertex connected to $0, 0, 1, 0, 0, 1$ is not connected to $(0, 1, 0, 0, 1, 0)$, as well as $1, 0, 0, 1, 0, 0)$. Thus, the graph with roots as the rotation set of $(0, 0, 1, 0, 0, 1)$ are disconnected and has tree connected components with is rooted at one of the rotation set of $(0, 0, 1, 0, 0, 1)$.

In conclusion, each root in Figure 5 is leading a connected component in G and all those components are isolated to each other. Since those roots are isomorphic to each other, according to how we define the flip operation in G, those six components follow the same isomorphic rule. □

Since six components are isomorphic, it is sufficient to study one piece, which is rooted at $(0, 0, 1, 0, 0, 1)$, denoted as D.

Claim 6. *Graph D has the following properties:*

(a) D is acyclic.

(b) D is graded.

Proof. (a). Since the complexity in D is increased by each flip, there is no flip operation sequence that could visit a configuration twice. So D has no cycle.

(b). The distance from one vertex to the root is consistent for different generating paths. □

To make Flip Graph capable of revealing the structure of primitive integer configurations , we are interested in the correspondence between primitive integer configurations and vertices in Flip Graph. Like the Calkin-Wilf tree is introduced, we expect Flip Graph G performances similarly – containing that one-to-one correspondence.

With those angles sum properties in Proposition 2, we could prove that each primitive configuration must show up in Flip Graph G. Equivalently, each primitive integer configuration is reached by a sequence of valid flip operations from a root configuration in Figure 5.

Claim 7. *Every integer configuration* $(\theta_1, \theta_2, \cdots, \theta_6)$ *with* $\sum \theta_i > 0$ *and* $gcd(\theta_1, \theta_2, \cdots, \theta_6) = 1$*, is reached by one of the three rotations of* $(0, 0, 1, 0, 0, 1)$.

Proof. Consider any primitive integer configuration θ with positive complexity. All the possible mountain-valley labellings for a valid hexagon is shown in Figure 6, according to [4].

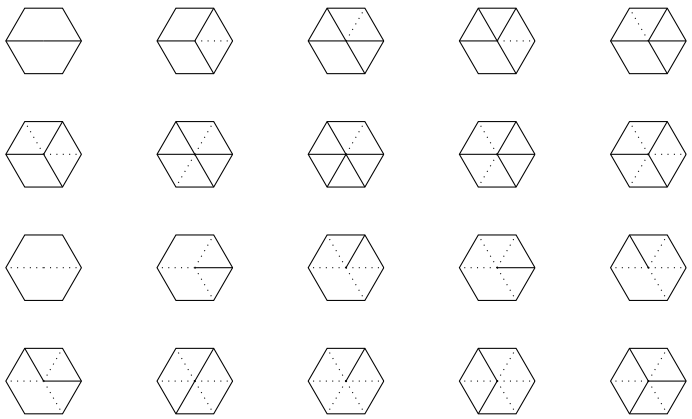

Figure 6: Mountain-valley labellings

If θ is a root, then it is in Flip Graph G.

If θ is not a root, then it must have a negative angle. Recursively applying the general Flip operation on $\theta's$ negative angle, there are only two possibilities:

a. generate a finite path with the end point as one of three rotations of $(0, 0, 1, 0, 0, 1)$,

b. generate an infinite path – visit infinite primitive configurations (consider repetitive visit)

If the path generated by negative flip operations is finite, consider the last primitive configuration γ on this path. If γ is a root, it falls under Case a. If γ is not a root, then it must have a negative angle which could reach a new primitive configuration. This contradicts γ being the last one in this path.

By Proposition 2(c), the general flip operation would preserve the sign of complexity. Here recursive flip operation is applied on negative angles, so the complexity is progressively decreasing. In that case the path could not revisit any configuration nor form an infinite path. So, Case b is not impossible when applying negative flip operation.

Now, under the condition, for any integer primitive configuration we could find a finite path from it to one of the roots by applying the flip operation on negative angles. While considering the inverse direction, each integer primitive configuration must be reached by one of the roots by the flip operation applying on positive angles, which is exactly what we defined in Flip Graph G. □

Claim 8. *Each vertex in Flip Graph G corresponds to a valid primitive integer configuration.*

Proof. In G, every root is a valid primitive integer configuration. All the vertices are connected by a sequence of flip operations starting from a root. By Proposition 1, every vertex in G must be a valid configuration on hexagon surface.

For primitiveness, the flip operation F and its inverse F^{-1} are associated with the same integer matrix M_i, which preserves common factors. Thus, any common factor on vertices in G should exist in root. Thus, the configuration corresponding to each vertex is primitive and integral. □

Combining last two claims, we reach an analogue to the Calkin-Wilf tree.

Claim 9 (Analogue to the Calkin-Wilf tree)**.** *Primitive integer configurations on the hexagon surface correspond one-to-one to the vertices in Flip Graph G, considering rotations and reflections.*

Proof. This is directly deduced by Claim 7 and 8. □

We gave out closed formulas for the number of vertices on each level and the number of mountain-valley configurations among them. By generating the Markov transition matrix, we calculated the limiting distribution for mountain-valley configurations.

4.2 Mountain-Valley Classification

According to Proposition 2 and Claim 9, configurations with positive complexity could not contain two consecutive negative fold angles. They must have the following configurations in Figure 7.

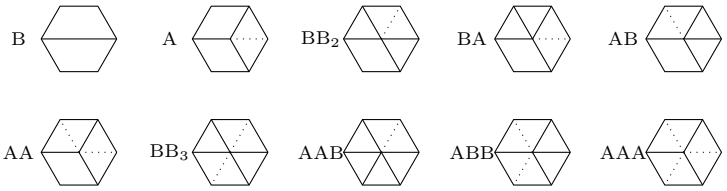

Figure 7: Mountain-valley labellings with positive complexity

Given a mountain-valley type, the children generated in Flip Graph are certain, shown in Figure 8. Based on the mountain-valley transition relations, in the perspective of Markov transition process,

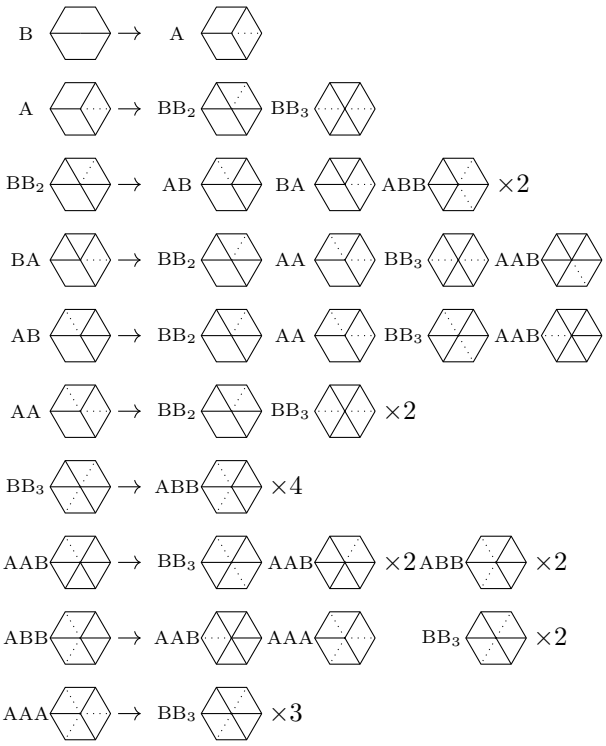

Figure 8: Flip images of configurations with positive complexity

the column-stochastic transition matrix for 3-dimensional configurations BB_3, AAB, ABB, AAA is

$$\begin{array}{c|cccc} & BB_3 & AAB & ABB & AAA \\ BB_3 & 0 & 0.2 & 0.5 & 1.0 \\ AAB & 0 & 0.4 & 0.25 & 0 \\ ABB & 1.0 & 0.4 & 0 & 0 \\ AAA & 0 & 0 & 0.25 & 0 \end{array},$$

with eigenvector $v = \begin{bmatrix} 0.33 \\ 0.17 \\ 0.4 \\ 0.1 \end{bmatrix}$ corresponding to the dominant eigenvalue $\lambda = 1$. Thus the final distribution for those mountain-valley configurations is consistent with v.

Claim 10. *The 3-dimensional areas' ratio in the null cone of [4] is*

$$BB_3 : AAB : ABB : AAA = 0.33 : 0.17 : 0.4 : 0.1.$$

Consider the isolated component D with the root $(1, 0, 0, 1, 0, 0)$. Recall Claim 6, Graph D is graded. As a result, we could group nodes by layer, where

$$\{\text{nodes on layer } n\} = \{\text{nodes which need } n \text{ flips to reach a root node}\}.$$

Mountain-valley configuration is a good tool to help classifying vertices on Graph D. We have discussed how flip operation works on mountain-valley configurations. Since D is determined by roots and flip operation, we could calculate the number of vertices on each layer by discussing different mountain-valley configurations separately.

In the following context, we will focus on 3-dimensional configurations BB_3, AAB, ABB, AAA on each layer.

Let

$$type(n) = \#\{\text{nodes of } type \text{ on layer } n\}, \text{where } type{=}BB_3, AAB, ABB, AAA.$$

To go from layer n to layer $n+1$, the number of children nodes is determined by mountain-valley type, as well as mountain-valley type of children. Also, some children are counted multiple times, because they have more than one parent node.

Proposition 6. *Each configuration in Graph $\mathcal{D}$ has k parents, where k is the number of negative fold angles it has.*

Proof. By doing the inverse flip operation of a negative angle in a configuration $\mathcal{C}$, we could generate another node in Graph $\mathcal{D}$, denoted by $\mathcal{P}$. By how we defined parent-child relationship in Definition 3, $\mathcal{P}$ must be a valid parent for $\mathcal{D}$. Most importantly, according to Proposition 5(c), all the parent nodes $\mathcal{C}$ reached would not overlap. Thus the number of negative angles in $\mathcal{C}$ indicates the number of parents it has in graph $\mathcal{D}$. □

$$\#\left\{\text{children in layer n+1}\right\} = \begin{pmatrix} 2_{BB_3}(n+1) \\ {}_{AAB}(n+1) \\ 2_{ABB}(n+1) \\ 3_{AAA}(n+1) \end{pmatrix} = \begin{pmatrix} 0 & 1 & 2 & 3 \\ 0 & 2 & 1 & 0 \\ 4 & 2 & 0 & 0 \\ 0 & 0 & 1 & 0 \end{pmatrix} \begin{pmatrix} {}_{BB_3}(n) \\ {}_{AAB}(n) \\ {}_{ABB}(n) \\ {}_{AAA}(n) \end{pmatrix}$$

$$\Rightarrow \begin{pmatrix} {}_{BB_3}(n+1) \\ {}_{AAB}(n+1) \\ {}_{ABB}(n+1) \\ {}_{AAA}(n+1) \end{pmatrix} = \begin{pmatrix} 0 & 1/2 & 1 & 3/2 \\ 0 & 2 & 1 & 0 \\ 2 & 1 & 0 & 0 \\ 0 & 0 & 1/3 & 0 \end{pmatrix} \begin{pmatrix} {}_{BB_3}(n) \\ {}_{AAB}(n) \\ {}_{ABB}(n) \\ {}_{AAA}(n) \end{pmatrix}$$

Figure 9: Transitions among 3-dimensional configurations

Claim 11. *The layer-counting transition matrix for 3-dimensional configurations is*

$$\begin{bmatrix} 0 & 1/2 & 1 & 3/2 \\ 0 & 2 & 1 & 0 \\ 2 & 1 & 0 & 0 \\ 0 & 0 & 1/3 & 0 \end{bmatrix}.$$

More generally, if we consider all the mountain-valley types in Figure 7, we have the general layer-counting transition matrix H as

$$H = \begin{bmatrix} 0 & 0 & 0 & 0 & 0 & 0 & 0 & 0 & 0 & 0 \\ 1 & 0 & 0 & 0 & 0 & 0 & 0 & 0 & 0 & 0 \\ 0 & 1 & 0 & 1 & 1 & 1 & 0 & 0 & 0 & 0 \\ 0 & 0 & 1 & 0 & 0 & 0 & 0 & 0 & 0 & 0 \\ 0 & 0 & 1 & 0 & 0 & 0 & 0 & 0 & 0 & 0 \\ 0 & 0 & 0 & 1 & 1 & 0 & 0 & 0 & 0 & 0 \\ 0 & 1/2 & 0 & 1/2 & 1/2 & 1 & 0 & 1/2 & 1 & 3/2 \\ 0 & 0 & 0 & 1 & 1 & 0 & 0 & 2 & 1 & 0 \\ 0 & 0 & 1 & 0 & 0 & 0 & 2 & 1 & 0 & 0 \\ 0 & 0 & 0 & 0 & 0 & 0 & 0 & 0 & 1/3 & 0 \end{bmatrix}$$

Proposition 7. *The growing complexity for number of nodes in each layer is $O(t^n)$, where t is the dominant eigenvalue for H, $t = 1 + \sqrt{3}$.*

5 Pythagorean 4-Tuples

In the proof of Proposition 2, an equivalent transformation is noteworthy.

$$Y \cong \begin{cases} x_1^2 + x_3^2 + x_5^2 = (x_1 + x_2 + x_3)^2 \\ x_1 + x_2 = x_4 + x_5 \\ x_2 + x_3 = x_5 + x_6 \end{cases}.$$

If we set $r = x_1 + x_2 + x_3$, then (x_1, x_3, x_5, r) satisfying $x_1^2 + x_3^2 + x_5^2 = r^2$ uniquely determines a valid hexagon configuration with parametrization

$$\begin{aligned} x_1 &= x_1 \\ x_3 &= x_3 \\ x_5 &= x_5 \\ x_2 &= r - x_1 - x_3 \\ x_4 &= r - x_3 - x_5 \\ x_6 &= r - x_1 - x_5. \end{aligned}$$

When considering integer configurations, Pythagorean 4-tuples should be gazed.

Definition 4 (Pythagorean 4-tuples)**.** (x_1, x_2, x_3, x_4) *is a (primitive)* Pythagorean 4-tuple *if x_1, x_2, x_3, x_4 are integers satisfying*

$$x_1^2 + x_2^2 + x_3^2 = x_4^2, \qquad \gcd(x_1, x_2, x_3, x_4) = 1, \qquad \textit{and} \qquad x_4 > 0.$$

According to Cass and Arpaia [2], on Pythagorean 4-tuples, there is an action by sign changes and the matrix A_4

$$A_4 = \begin{bmatrix} 0 & -1 & -1 & 1 \\ -1 & 0 & -1 & 1 \\ -1 & -1 & 0 & 1 \\ -1 & -1 & -1 & 2 \end{bmatrix},$$

which generates other complicated Pythagorean 4-tuples from simpler ones. For example, A_4 could send $(3, -2, -6, 7)$ to $(15, 10, 6, 19)$,

$$\begin{pmatrix} 0 & -1 & -1 & 1 \\ -1 & 0 & -1 & 1 \\ -1 & -1 & 0 & 1 \\ -1 & -1 & -1 & 2 \end{pmatrix} \begin{pmatrix} 3 \\ -2 \\ -6 \\ 7 \end{pmatrix} = \begin{pmatrix} 15 \\ 10 \\ 6 \\ 19 \end{pmatrix}$$

5.1 Pythagorean Graph

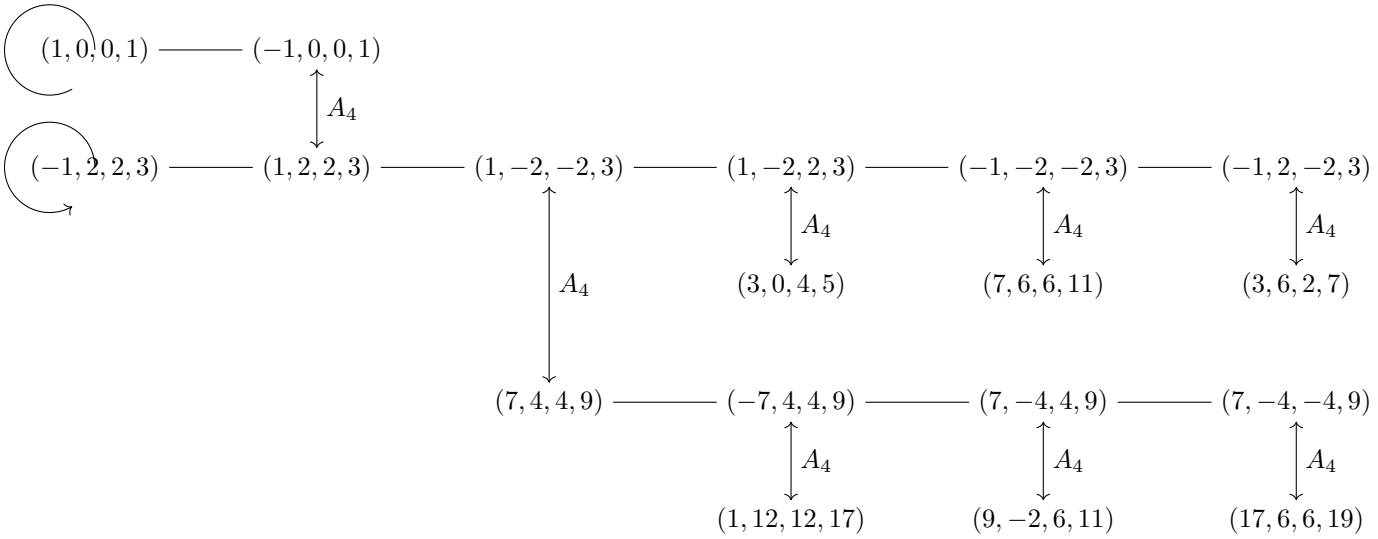

5.2 Connection to Hexagon Configuration

For one hexagon configuration $(\theta_1, \theta_2, \cdots, \theta_6)$, it has two representations in terms of Pythagorean 4-tuples: $(\theta_1, \theta_3, \theta_5, r_{odd})$ and $(\theta_2, \theta_4, \theta_6, r_{even})$.

$$(\theta_1, \theta_3, \theta_5, r_{odd}) \quad \leftrightarrow \quad \begin{matrix} r_{odd}-\theta_1-\theta_3 & & \theta_1 \\ & \theta_3 \quad \bigcirc \quad r_{odd}-\theta_1-\theta_5 & \\ r_{odd}-\theta_3-\theta_5 & & \theta_5 \end{matrix} \tag{5}$$

$$(\theta_2, \theta_4, \theta_6, r_{even}) \quad \leftrightarrow \quad \begin{matrix} \theta_2 & & r_{even}-\theta_6-\theta_2 \\ & r_{even}-\theta_4-\theta_2 \quad \bigcirc \quad \theta_6 & \\ \theta_4 & & r_{even}-\theta_4-\theta_6 \end{matrix} \tag{6}$$

The Pythagorean tuples in (5) and (6) are related by matrix A_4.

More explicitly, if we set (a, b, c, r) as a representation of a configuration, then the other equivalent representation would be $(r-b-c, r-a-c, r-a-b, 2r-a-b-c)$, which is obtained by rotating the first configuration by 180 degree. Those two 4-tuple representations are connected by A_4.

Now we only consider odd-angle representation. For a pythagorean 4-tuple (a, b, c, r), we define the corresponding hexagon configuration as $(\theta_1 = a, \theta_2 = r-a-b, \theta_3 = b, \theta_4 = r-b-c, \theta_5 = c, \theta_6 = r-a-c)$.

Theorem 2. *Restricted under odd-angle representation, there is a bijection between primitive pythagorean 4-tuples and integer hexagon configurations.*

5.2.1 Flip Operation

We denote a sign change operation on pythagorean group as s_{2i-1} if it is changing the sign of the x_i.

If we apply a sign change s_k on the pythagorean 4-tuple, we have a corresponding Flip operation F_k on the hexagon configuration with odd angles θ_1, θ_3, or θ_5. If we have a composition of $A_4 \circ s_k \circ A_4$, then the corresponding transition in hexagon configuration is flipping a even angle, i.e. $\theta_2, \theta_4, \theta_6$. More specifically, we have $A_4 \circ s_k \circ A_4$ correspond to $F_{(k+3) \mod 6}$.

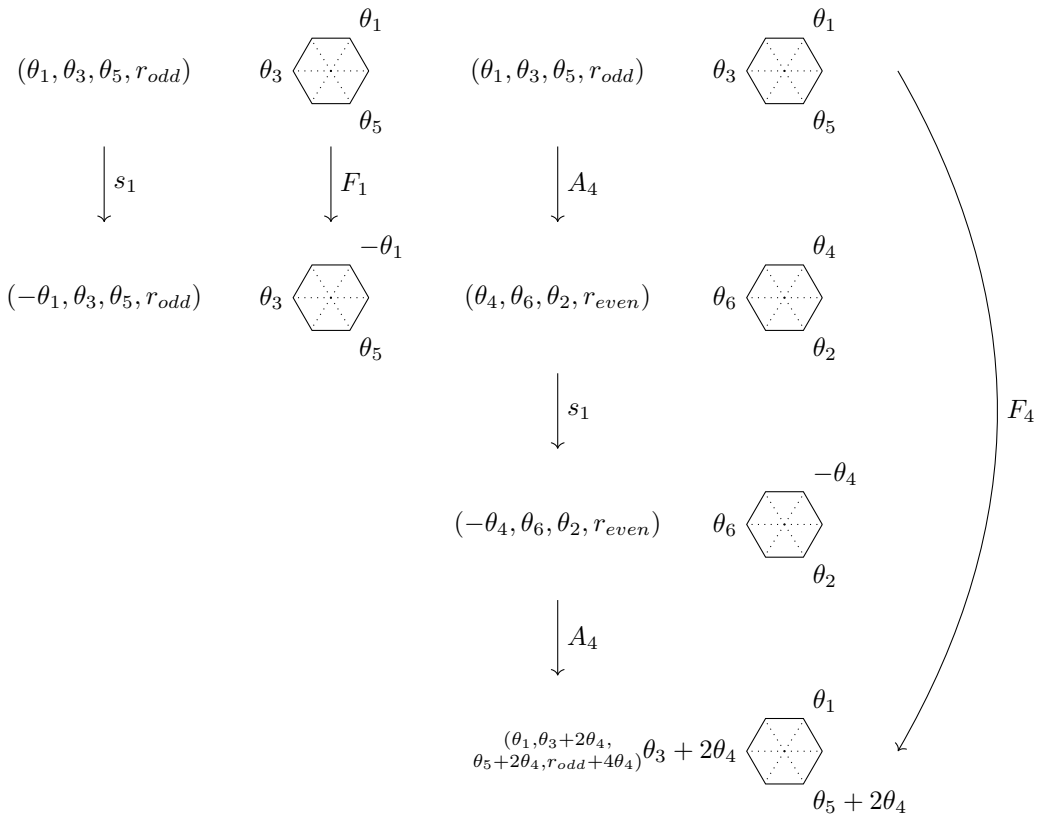

Figure 10: Operations correspondence between Pythagorean 4-tuple and hexagon configuration

The bijection map for operations reveals the structure of pythagorean tuple. We consider the 4-tuple set $\mathcal{R} = \{(1,0,0,1), (0,1,0,1), (0,0,1,1)\}$.

Claim 12. *Every pythagorean primitive* 4*-tuple could be reached by one element of* R *if they have the same parity.*

5.2.2 Pythagorean Graph $\mathcal{H}$ and Hexagon Flip Graph $\mathcal{G}$

To give out a more simple statement about the connection between pythagorean 4-tuple and hexagon configuration, we define a graph $\mathcal{H}$ representing operations and tuples as follows:

Definition 5 (Restricted graph)**.** *In graph* $\mathcal{H}$*, the primitive* 4*-tuple* $(1,0,0,1)$*, denoted as* r*, is a node in* $V(\mathcal{H})$*. If a pythagorean* 4*-tuple is generated by the composition of a sequence of operations* s_i *and* A_4*, it is representing a node in* $V(\mathcal{H})$*.* s_i *will only change* ***one*** *element's sign and could only be applied to a positive value.*

The hexagon flip graph G and the Pythagorean 4-tuple graph H can be related by constructing a graph K which has graph-theoretic maps $\mathcal{K} \to \mathcal{G}$ and $\mathcal{K} \to \mathcal{H}$. The graph $\mathcal{K}$ has twice as many vertices as $\mathcal{G}$ and $\mathcal{H}$, in the sense that $\mathcal{K} \to \mathcal{G}$ and $\mathcal{K} \to \mathcal{H}$ are 2-to-1 on vertices. (G and H have the "same number" of vertices, i.e. there are two natural bijections between vertices of G and vertices of H, the odd-angle and even-angle maps.)

The relation to get from $\mathcal{G}$ to $\mathcal{K}$ is replacing each vertex with an edge and two vertices.

The relation to get from $\mathcal{H}$ to $\mathcal{K}$ is known as a "double cover" (or "degree 2 cover")

References

[1] D. J. Balkcom and M. T. Mason, *Robotic origami folding*, The International Journal of Robotics Research, 27 (2008), pp. 613–627.

[2] D. Cass and P. J. Arpaia, *Matrix generation of pythagorean n-tuples*, Proceedings of the American Mathematical Society, 109 (1990), pp. 1–7.

[3] B. G.-g. Chen and C. D. Santangelo, *Branches of triangulated origami near the unfolded state*, Physical Review X, 8 (2018), p. 011034.

[4] A. Cuza, Y. Liu, and O. Saeed, *Origami on lattices*, (2019).